NIH Public Access
Author Manuscript
Calcif Tissue Int. Author manuscript; available in PMC 2012 July 1.

Published in final edited form as:
Calcif Tissue Int. 2011 July ; 89(1): 43–52. doi:10.1007/s00223-011-9492-2.

Three-Dimensional Evaluation of Mandibular Bone Regenerated By Bone Transport Distraction Osteogenesis

Elias Kontogiorgos,
Department of Biomedical Sciences, Texas A&M Health Science Center, Baylor College of Dentistry, 3302 Gaston Avenue, Dallas, TX 75246, USA

Mohammed E. Elsalanty,
Department of Oral Biology, School of Dentistry, Georgia Health Science University, Augusta, GA, USA

Uriel Zapata,
Department of Biomedical Sciences, Texas A&M Health Science Center, Baylor College of Dentistry, 3302 Gaston Avenue, Dallas, TX 75246, USA

Ibrahim Zakhary,
Department of Oral Biology, School of Dentistry, Georgia Health Science University, Augusta, GA, USA

William W. Nagy,
Department of Restorative Sciences, Texas A&M Health Science Center, Baylor College of Dentistry, Dallas, TX, USA

Paul C. Dechow, and
Department of Biomedical Sciences, Texas A&M Health Science Center, Baylor College of Dentistry, 3302 Gaston Avenue, Dallas, TX 75246, USA

Lynne A. Opperman
Department of Biomedical Sciences, Texas A&M Health Science Center, Baylor College of Dentistry, 3302 Gaston Avenue, Dallas, TX 75246, USA

Elias Kontogiorgos: ekontogiorgos@bcd.tamhsc.edu; Mohammed E. Elsalanty: melsalanty@georgiahealth.edu; Uriel Zapata: uzapata@eafit.edu.co; Ibrahim Zakhary: izakhary@georgiahealth.edu; William W. Nagy: wnagy@bcd.tamhsc.edu; Paul C. Dechow: pdechow@bcd.tamhsc.edu; Lynne A. Opperman: lopperman@bcd.tamhsc.edu

Abstract

The purpose of this study was to evaluate the structure and material properties of native mandibular bone and those of early regenerate bone, produced by bone transport distraction osteogenesis. Ten adult foxhounds were divided into two groups of five animals each. In all animals, a 3- to 4-cm defect was created on one side of the mandible. A bone transport reconstruction plate, consisting of a reconstruction plate with an attached intraoral transport unit, was utilized to stabilize the mandible and regenerate bone at a rate of 1 mm/day. After the distraction period was finished, the animals were killed at 6 and 12 weeks of consolidation. Micro-computed tomography was used to assess the morphometric and structural indices of regenerate bone and matching bone from the unoperated contralateral side. Significant new bone was formed within the defect in the 6- and 12-week groups. Significant differences ($P \leq 0.05$) between

© Springer Science+Business Media, LLC 2011

Present Address: U. Zapata, Departamento de Ingeniería Mecánica, Universidad Eafit, Carrera 49 No 7 Sur - 50, Medellin, Colombia

M. Elsalanty and L. Opperman are co-owners of Craniotech ACR Devices, LLC. All other authors have stated no conflict of interest.

NIH-PA Author Manuscript
NIH-PA Author Manuscript
NIH-PA Author Manuscript

NIH-PA Author Manuscript

NIH-PA Author Manuscript

NIH-PA Author Manuscript

mandibular regenerated and native bone were found in regard to bone volume fraction, mineral density, bone surface ratio, trabecular thickness, trabecular separation, and connectivity density, which increased from 12 to 18 weeks of consolidation. We showed that regenerated bone is still mineralizing and that native bone appears denser because of a thick outer layer of cortical bone that is not yet formed in the regenerate. However, the regenerate showed a significantly higher number of thicker trabeculae.

Keywords

Micro-computed tomography; Distraction device; Bone transport; Bone regeneration

The possibility of bone lengthening by means of distraction osteogenesis was suggested many years ago by Codivilla [1] and later clinically and biologically established by Ilizarov [2]. Their experiments were focused on long bones; however, during the past two decades the same principles were applied to the maxillofacial region for the correction of severe craniofacial malformations [3–5] as well as to achieve alveolar ridge augmentation [6–8]. A recent development in the area is the application of the distraction osteogenesis concept to correct bone defects of the lower jaw [9, 10].

Segmental mandibular bone defects can result from surgical excision of hard and soft tissues due to tumor, blast injuries, high-impact trauma, or repeated surgical debridements for treatment of chronic osteomyelitis of the mandible. Distraction osteogenesis is intended to restore the appearance and the physiology of the affected area.

It is now possible to reconstruct mandibular bone defects successfully and to ensure that a great amount of esthetics and functioning is restored [11, 12]. Certain reconstructive methods enable these kinds of goals to be achieved. They require bone stabilization, which is achieved by a titanium plate fixed at the borders of the defect and can be enhanced with bone grafting. In the case of using only the reconstructive plate without bone grafting, the esthetic outcome is usually acceptable but functional rehabilitation of the patient becomes extremely difficult since the prosthodontic reconstruction is impossible. This state has a pronounced negative effect on the patient's quality of life. On the other hand, bone-grafting procedures have been successfully used during recent decades, including vascularized [13, 14], nonvascularized [15, 16], and bone substitutes (e.g., calcium phosphate ceramics and bioglasses) [17, 18]. There is a preference for vascularized bone grafts because of their higher success rates compared with nonvascularized ones [19, 20]. These grafted tissues can be used for endosseous implant placement and subsequent dental restoration, providing a good clinical outcome [21–23].

Despite the high success of bone grafting, some significant complications have been reported, most importantly donor site morbidity, graft resorption, and relapse [24–26]. These difficulties have led to the exploration of new ways to reconstruct mandibular bone defects. A recent development in this field, by Elsalanty et al. [27], is using newer, more sophisticated devices for reconstructing the bone in the mandible via bone transport osteogenesis principles. A new device, the mandibular bone transport reconstruction plate (BTRP), is an intraoral apparatus capable of producing new bone as it slides on a titanium reconstruction plate. The resulting regenerated bone is not substantially different from preexisting mandibular bone, and it can eventually provide a suitable substrate for endosseous implant placement to support potential prosthodontic appliances, but no existing studies have examined the feasibility of this approach.

NIH-PA Author Manuscript

NIH-PA Author Manuscript

NIH-PA Author Manuscript

Implant osseointegration is directly related to bone quantity and quality. So far, little is known about the quality and quantity of the regenerated bone or the maintenance of successful continuity with the existing bone at the defect borders. In addition, it is not clear when the regenerated bone is biomechanically able to function under the variable loads of mastication and to begin the dental restorative procedures.

The aims of this research project were (1) to characterize the quality of the newly formed bone and determine the bone area fraction in the distraction region and (2) to investigate the bone structure and material properties of the regenerate left to consolidate for either 12 or 18 weeks.

Materials and Methods

In this study, bone transport osteogenesis reconstruction of a canine mandibular defect model was used. In each animal, a defect much larger than a critical-sized defect was created (30–40 mm). A BTRP (Craniotech ACR Devices, Dallas, TX) was used to create regenerated bone across the gap, using standard distraction osteogenesis criteria.

Animals

Ten adult foxhounds were divided into two groups of five animals each. Following the distraction period, implants were placed in the regenerate after 6 weeks of consolidation. Implants placed in the contralateral side of the mandible served as controls. After the implants were inserted, group A was left to heal for 6 weeks and group B for 12 weeks.

Surgical Procedure and Distraction Protocol

The use of the device, surgical technique, and distraction protocol were conducted using a Baylor College of Dentistry–approved Institutional Animal Care and Use Committee protocol, as described previously [27]. Briefly, all surgical procedures were done under general anesthesia. For anesthesia, each dog was injected with atropine 2 mg/100 lb SQ b 15 min before surgery, followed by diazepam 0.5 mg/kg IM. When the animal was sedated, isoflurane was administered via a mask at 4% in 100% O_2 with a flow rate of 3–4 L per minute. Next, endotracheal intubation was carried out (tube size 10), and animals were maintained on isoflurane at 1–2% in 100% O_2 at a flow rate of 0.5–2 L per minute, depending on the tidal volume [27]. To create the bone defect, bone was excised with the use of a surgical reciprocating mini-saw (Stryker Craniomaxillofacial, Portage, MI), leaving a defect of 3–4 cm in length. The periosteum was preserved over the bone stumps. The mandible was stabilized with the titanium reconstruction plate positioned on the buccal side. This plate has its middle segment manufactured as a transport track. The two ends of the plate were stabilized to the bone segments by three or four 2.7-mm titanium screws on either side of the defect. The bone transport segment was separated from the posterior bone stump, with care taken to preserve the outer periosteum and the nerve and blood vessels in the alveolar canal, and the device was secured on it (buccal side) via six 1.7-mm titanium screws. The bone transport segment measured about 15 mm in the mesial–distal direction. Wound closure was achieved in three layers using 3-0 Vicryl sutures. After surgery, the animals were given buprenorphine at 0.005 mg/kg SQ every 12 h for pain. Food and water consumption was monitored daily to assure proper nutrition. Advancement of the transport segment was carried out by clockwise rotation of the activation cable, which extruded through the skin behind the mandibular ramus.

Distraction started on the fifth postoperative day and progressed at a rate of 1 mm per day divided into two activations every 12 h, until the transport segment docked against the opposite end of the defect (Fig. 1a, b). The activation cable that protruded through the skin

NIH-PA Author Manuscript

NIH-PA Author Manuscript

NIH-PA Author Manuscript

wound was kept clean and monitored daily. The progress of the distraction and consolidation was assessed through weekly radiographs.

After 2 weeks of distraction osteogenesis on the experimental side, the mandibular premolars and first premolar of the contralateral (control) side were extracted (Fig. 2a). Following tooth removal, the soft tissues were repositioned and closed with interrupted sutures. After another 2 weeks, distraction osteogenesis was completed. Consolidation of the regenerate lasted for 6 weeks, followed by implant placement (Figs. 1c, 2b). Three implants (Straümann, Basel, Switzerland; Standard Plus Implant, diameter 3.3 mm, length 8 mm) were placed in the experimental side and three on the control side. Recipient sites were exposed by elevation of mucoperiosteal flaps. The sites were prepared under copious irrigation with sterile physiologic saline using standard commercially available drills for the implant type. For the control implants the thread was tapped into the bone cavity, while for the regenerate implants tapping was not necessary. Healing abutments were secured, and primary wound closure was achieved with nonresorbable sutures. Group A was left to heal for an additional 6 weeks and group B for 12 weeks.

Animals were killed using Beuthanasia-D (Intervet/Schering-Plough Animal Health, Summit, NJ; 1 cc IC while under anesthesia) in accordance with the recommendations of the Panel on Euthanasia of the American Veterinary Medical Association, and the mandibles were dissected. Bone specimens were collected from the regenerate and the control sides. Specimens were fixed in 10% buffered formalin (10% SBF) [28] for 2 weeks.

Micro-Computed Tomography

Bone specimens were scanned at 20-μ voxel size resolution (micro-CT 35; Scanco Medical, Zurich, Switzerland). The scanning settings were as follows: X-ray energy levels at 70 kVp, current at 114 μA, and integration time at 800 ms with 1,000 projections per 180°. Figures 1d and 2b show the volume of interest (VOI) created from 150 slices each for the experimental and control sides, respectively. After scanning, the reconstructed data were segmented using a threshold algorithm that was held constant for all analyses. Because the bone specimens were intact, the outer cortical bone was digitally separated from the inner trabecular bone by contouring the outline manually. Using the company's software (Image Processing Language, Scanco), two analyses were performed for every bone sample, one for the cortical and one for the trabecular segment. For the regenerate specimens, the cortical bone was so thin that it was not possible to separate it from the trabecular bone, so only the analysis for trabecular bone was performed for the regenerate. Bone volume fraction (BV/TV, where BV is bone volume and TV is total volume), density (mgHA/cm^3), trabecular thickness (Tb.Th), trabecular separation (Tb.Sp), trabecular number (Tb.N), and connectivity density (Conn.D) were calculated for all samples.

Histologic Analysis

After completion of the micro-computed tomographic (micro-CT) analysis, specimens were processed for non-decalcified histologic evaluation [29]. First, they were dehydrated using a series of ethanol baths of increasing concentrations (from 70% to 100%), followed by embedding in methyl methacrylate. Diamond disks (Isomet; Buehler, Lake Bluff, IL) were used to section the specimens in a buccal to lingual orientation. Next, the sections were ground down with 240, 320, 400, and 600 grit polishers (Handimet2, Buehler) and further polished with 0.05 μm paste. Stevenel blue and fuchian red were used to stain cells and tissues. Images were captured with a digital camera (Olympus, Center Valley, PA).

NIH-PA Author Manuscript

NIH-PA Author Manuscript

NIH-PA Author Manuscript

Statistical Analysis

A repeated-measure ANOVA was used to detect differences between the control and experimental sides within the same animal, the same group, and between the two groups, using a statistical software package (SPSS v.17; SPSS Inc., Chicago, IL). Significance was set at $P < 0.05$. Equality of the variances of the differences between levels of each repeated factor was tested using Mauchly's sphericity test. The Kolmogorov–Smirnov test was used to confirm normality of the residuals. To determine whether there were pathologic changes in bone structure that were different from the normal change associated with a change in volume fraction, linear regression models were used for each of the bone morphometric indices vs. the volume fraction between control and regenerate bone.

Results

Histologic examination of the regenerated bone noted mainly trabecular bone surrounded by a thin cortical area. There was a central region with numerous blood vessels, nerves, and fibrous tissue that was comparable to the inferior alveolar canal and associated neurovascular bundle of the control side (Fig. 3). This finding was consistent in all histologic slides examined.

For the micro-CT analysis, the region of interest of every specimen was 150 slices at a resolution of 20 μ, resulting in a 3D area of 3 mm in length and approximately 45 mm in height (Fig. 4). Results from micro-CT analysis are presented in Table 1. Comparison of the overall bone (cortical and trabecular bone together) between the two consolidation time periods (week 12 vs. week 18) showed that TV and BV did not differ. However, there was an increase in the apparent density (App.D), material density (Mtr.D), and BV/TV. For trabecular bone only, the volume fraction (Tb.BV/TV), the bone surface ratio (Tb.BS/BV), Conn.D, Tb.N, Tb.Th, and Tb.Sp were not different between the two groups.

Analysis of the overall bone according to tissue type (control vs. regenerate) within the same animal revealed that App.D, Mtr.D, and BV/TV were significantly higher for the control tissue. For trabecular bone Tb.BV/TV, Conn.D, and Tb.Th were significantly higher for the regenerate tissue and Tb.BS/BV and Tb.Sp were significantly less for the regenerate tissue.

Analysis of the overall bone according to the combined effect of tissue type and consolidation time showed that TV and BV of the regenerate tissue significantly increased and reached the same level as the control tissue at 18 weeks. App.D and BV/TV increased for both tissue types, with the control showing higher values. Mtr.D for the control tissue did not change, but for the regenerate tissue it showed a significant increase at 18 weeks but did not reach the level of the control. Examining the trabecular bone of the control tissue, Tb.BV/TV, Tb.BS/BV, Conn.D, Tb.N, Tb.Th, and Tb.Sp did not change from 12 to 18 weeks. In contrast, the regenerate tissue demonstrated an increase in Tb.BV/TV and Tb.Th, a decrease in Tb.BS/BV and Tb.Sp, and no change in Conn.D and Tb.N from 12 to 18 weeks.

The regression analysis of the bone morphometric indices against bone volume fraction is shown in Table 2 and Fig. 5. Accordingly, the analysis of App.D against BV/TV showed a strong positive correlation for both tissue types; however, the analysis of Mtr.D against BV/TV showed no correlation for the control tissue and a moderate correlation for the regenerate tissue. In trabecular bone, both tissue types demonstrated a strong correlation of Tb.BS/BV against Tb.BV/TV. The control tissue showed a moderate correlation of Conn.D and a strong correlation for Tb.N, Tb.Th, and Tb.Sp against Tb.BV/TV. In contrast, the regenerate tissue showed no significant correlation for Conn.D and Tb.N and a strong

NIH-PA Author Manuscript

NIH-PA Author Manuscript

NIH-PA Author Manuscript

correlation for Tb.Th and Tb.Sp against Tb.BV/TV. Because of the small sample size (n = 10), comparison of the regression slope between the two tissue types was not possible.

Discussion

Bone mineral density is the most important determinant factor of bone strength [30, 31]. We found that regenerated mandibular bone continued to mineralize from 12 to 18 weeks of consolidation time, but it had not reached the levels of control bone. Micro-CT analysis provides two separate indices that assess mineral density: apparent and material density, which are inversely related to volume. For apparent density the denominator is total volume, whereas for material density the denominator is bone volume. In our study total and bone volume increased between 12 and 18 weeks and apparent and material density increased as well. This finding indicates a high mineralization rate of regenerated bone between 12 and 18 weeks of consolidation time. Regenerated bone has thicker, denser, and more numerous trabeculae than native bone. However, the architecture of the regenerated bone was mainly trabecular, with an outer thin layer of cortical bone, whereas the control bone demonstrated well-defined cortical and trabecular bone regions. This explains why the overall bone volume fraction of the regenerated bone was less than the control, yet the trabecular level appeared denser. Regression analysis of the bone surface/volume ratio against bone volume fraction showed no difference between regenerated and control bone, indicating that there are no pathological changes in the regenerate bone structure associated with a change in volume fraction.

Micro-CT analysis of bone tissue does not give insight into the cell population, mineral apposition rate, and bone remodeling as bone histomorphometry does. However, it is a validated method for 3D quantitative structural analysis of bone [32]. Previous histomorphometric evaluations in a canine model found that mineralization of the mandibular regenerate increased only up to week 4 of consolidation and the trabecular number increased up to week 8 [33]. However, that study focused on mandibular lengthening, and the evaluation was in two dimensions (histology). Our results demonstrated that mineralization continues up to week 18 of consolidation and that trabecular number was stable from 12 to 18 weeks. Trabecular thickness increased and trabecular separation decreased, giving the regenerated bone a denser appearance. Connectivity density, which reflects the number of trabeculae that can be cut without separating the trabecular mesh, was significantly higher for the regenerated bone. Whether or not this bone index correlates with the biomechanical properties and quality of bone is debatable [34–36].

Mineralization of the regenerated bone begins from the proximal ends and continues toward the center [37, 38], and the amount of mineralization differs according to the region within the same specimen [39, 40]. This means that choosing the VOI and the threshold level has considerable consequences. First, choosing a uniform VOI of homologous regions throughout one study is essential if a structural comparison of the specimens is desired. In our study 150 slices of mandibular bone between the anterior and middle implants were chosen for the control and regenerate sides. Second, the difficulty in choosing the correct threshold level is that bone, especially regenerated bone, is nonhomogenous, with trabeculae of varying densities. Using a uniform threshold does not account for the possible density variations. On the other hand, choosing an adaptive threshold does not allow for comparisons of different specimens in a given study because a 10% change in the threshold results in a 5% change in bone volume fraction [32, 41]. For that reason it has been proposed that it is safe to use a uniform threshold to compare normal with osteoporotic bone, if high resolution (20 μ or less) is achieved [32]. In our study the resolution was set to 20 μ and a uniform threshold for all specimens was utilized.

NIH-PA Author Manuscript

NIH-PA Author Manuscript

NIH-PA Author Manuscript

The characterization of trabecular bone according to plate-like and rod-like structure is based on the structural model index (SMI) [42]. A value of 3 indicates a rod-like structure, and a value of 0 indicates a plate-like structure; but the appearance of regenerated mandibular bone is different from the native one because of increased bone remodeling. Trabecular plates are perforated and connecting rods are dissolved, so traditional histomorphometric procedures, which are based on a fixed model type, might lead to questionable results [43]. This is supported by the negative SMI values that were observed for the regenerate bone because of the difficulty in separating cortical bone from trabecular bone that led us to include the whole sample in the analysis. For the aforementioned reasons, we did not make any assumptions about the bone structure and the micro-CT measurements were based solely on 3D direct measurements.

Finally, a common finding with the micro-CT evaluation for all of the regenerated bone samples was a central region that was not mineralized, compared with control bone samples where a similar region was found close to the inferior margin of the mandible. Both of these nonmineralized regions were not included in the micro-CT analysis. This occurrence in the regenerate may have been caused in part by trauma and disruption of the healing process by the second surgery of dental implant placement after 6 weeks of consolidation. Another explanation is the regeneration of nerves and blood vessels from the inferior alveolar neurovascular bundle that was kept intact inside the transport disc. Histologic analysis showed that on the control side this zone corresponds to the inferior alveolar canal that houses the inferior alveolar nerve and vessels. For the regenerated side, newly formed blood vessels, nerves, and fibrous tissue were found in accordance with our previous study [27].

In conclusion, micro-CT analysis showed significant differences between mandibular regenerated and native bone with regard to mineral density and bone volume fraction after 12 and 18 weeks of consolidation. We showed that regenerated bone is still mineralizing and that native bone appears denser because of a thick outer layer of cortical bone that is not yet formed in the regenerate. However, the regenerate presents with a significantly higher number of thicker trabeculae, which contributes to its mechanical properties to withstand mastication loads. This is the first study that assesses the effect of consolidation period for mandibular bone transport distraction osteogenesis to regenerate bone after placement of dental implants. Future experiments will establish if extended consolidation time will cause the regenerated bone to reach the same level of material density as native bone and increase the thickness of its outer layer of cortical bone. Restoration of the dental implants with artificial teeth will allow testing of the effect of mastication loads on the regenerated bone structure and material properties.

Acknowledgments

The authors would like to thank Ms. Connie Tillberg for expert help with histologic preparations. We are grateful for the generous donation of implants from Straumann.

References

1. Codivilla A. The classic: on the means of lengthening, in the lower limbs, the muscles and tissues which are shortened through deformity. 1905. Clin Orthop Relat Res. 2008; 466:2903–2909. [PubMed: 18820986]
2. Ilizarov GA. Basic principles of transosseous compression and distraction osteosynthesis [in Russian]. Ortop Traumatol Protez. 1971; 32:7–15.
3. Carls FR, Sailer HF. Seven years clinical experience with mandibular distraction in children. J Craniomaxillofac Surg. 1998; 26:197–208. [PubMed: 9777498]
4. McCarthy JG, Schreiber J, Karp N, Thorne CH, Grayson BH. Lengthening the human mandible by gradual distraction. Plast Reconstr Surg. 1992; 89:1–10. [PubMed: 1727238]

NIH-PA Author Manuscript

NIH-PA Author Manuscript

NIH-PA Author Manuscript

5. Molina F, Ortiz Monasterio F. Mandibular elongation and remodeling by distraction: a farewell to major osteotomies. Plast Reconstr Surg. 1995; 96:825–840. [PubMed: 7652056]
6. Chiapasco M, Lang NP, Bosshardt DD. Quality and quantity of bone following alveolar distraction osteogenesis in the human mandible. Clin Oral Implants Res. 2006; 17:394–402. [PubMed: 16907770]
7. Chiapasco M, Romeo E, Vogel G. Vertical distraction osteogenesis of edentulous ridges for improvement of oral implant positioning: a clinical report of preliminary results. Int J Oral Maxillofac Implants. 2001; 16:43–51. [PubMed: 11280361]
8. Krenkel C, Grunert I. The Endo-Distractor for preimplant mandibular regeneration. Rev Stomatol Chir Maxillofac. 2009; 110:17–26. [PubMed: 19135219]
9. Elsalanty ME, Taher TN, Zakhary IE, Al-Shahaat OA, Refai M, El-Mekkawi HA. Reconstruction of large mandibular bone and soft-tissue defect using bone transport distraction osteogenesis. J Craniofac Surg. 2007; 18:1397–1402. [PubMed: 17993888]
10. Herford AS. Use of a plate-guided distraction device for transport distraction osteogenesis of the mandible. J Oral Maxillofac Surg. 2004; 62:412–420. [PubMed: 15085505]
11. Marx RE, Ehler WJ, Peleg M. “Mandibular and facial reconstruction” rehabilitation of the head and neck cancer patient. Bone. 1996; 19:59S–82S. [PubMed: 8830998]
12. Marx RE. Mandibular reconstruction. J Oral Maxillofac Surg. 1993; 51:466–479. [PubMed: 8478754]
13. Kuriloff DB, Sullivan MJ. Mandibular reconstruction using vascularized bone grafts. Otolaryngol Clin North Am. 1991; 24:1391–1418. [PubMed: 1792077]
14. Takushima A, Harii K, Asato H, Nakatsuka T, Kimata Y. Mandibular reconstruction using microvascular free flaps: a statistical analysis of 178 cases. Plast Reconstr Surg. 2001; 108:1555–1563. [PubMed: 11711927]
15. Branemark PI, Lindstrom J, Hallen O, Breine U, Jeppson PH, Ohman A. Reconstruction of the defective mandible. Scand J Plast Reconstr Surg. 1975; 9:116–128. [PubMed: 1103278]
16. Chow JM, Hill JH. Primary mandibular reconstruction using the AO reconstruction plate. Laryngoscope. 1986; 96:768–773. [PubMed: 3724329]
17. Marcacci M, Kon E, Zaffagnini S, Giardino R, Rocca M, Corsi A, Benvenuti A, Bianco P, Quarto R, Martin I, Muraglia A, Cancedda R. Reconstruction of extensive long bone defects in sheep using porous hydroxyapatite sponges. Calcif Tissue Int. 1999; 64:83–90. [PubMed: 9868289]
18. Oonishi H. Orthopaedic applications of hydroxyapatite. Biomaterials. 1991; 12:171–178. [PubMed: 1652293]
19. Foster RD, Anthony JP, Sharma A, Pogrel MA. Vascularized bone flaps versus nonvascularized bone grafts for mandibular reconstruction: an outcome analysis of primary bony union and endosseous implant success. Head Neck. 1999; 21:66–71. [PubMed: 9890353]
20. Pogrel MA, Podlesh S, Anthony JP, Alexander J. A comparison of vascularized and nonvascularized bone grafts for reconstruction of mandibular continuity defects. J Oral Maxillofac Surg. 1997; 55:1200–1206. [PubMed: 9371107]
21. Barber HD, Seckinger RJ, Hayden RE, Weinstein GS. Evaluation of osseointegration of endosseous implants in radiated, vascularized fibula flaps to the mandible: a pilot study. J Oral Maxillofac Surg. 1995; 53:640–645. [PubMed: 7776045]
22. Khatami AH, Toljanic JA, Kleinman A. Mandibular reconstruction with vascularized fibula flap and osseointegrated implants: a clinical report. J Oral Implantol. 2010; 36:385–390. [PubMed: 20545535]
23. Wei FC, Santamaria E, Chang YM, Chen HC. Mandibular reconstruction with fibular osteoseptocutaneous free flap and simultaneous placement of osseointegrated dental implants. J Craniofac Surg. 1997; 8:512–521. [PubMed: 9477839]
24. Ahlmann E, Patzakis M, Roidis N, Shepherd L, Holtom P. Comparison of anterior and posterior iliac crest bone grafts in terms of harvest-site morbidity and functional outcomes. J Bone Joint Surg Am. 2002; 84-A:716–720. [PubMed: 12004011]
25. Holzle F, Kesting MR, Holzle G, Watola A, Loeffelbein DJ, Ervens J, Wolff KD. Clinical outcome and patient satisfaction after mandibular reconstruction with free fibula flaps. Int J Oral Maxillofac Surg. 2007; 36:802–806. [PubMed: 17614257]

NIH-PA Author Manuscript

NIH-PA Author Manuscript

NIH-PA Author Manuscript

26. Zijderveld SA, ten Bruggenkate CM, van Den Bergh JP, Schulten EA. Fractures of the iliac crest after split-thickness bone grafting for preprosthetic surgery: report of 3 cases and review of the literature. J Oral Maxillofac Surg. 2004; 62:781–786. [PubMed: 15218554]
27. Elsalanty ME, Zakhary I, Akeel S, Benson B, Mulone T, Triplett GR, Opperman LA. Reconstruction of canine mandibular bone defects using a bone transport reconstruction plate. Ann Plast Surg. 2009; 63:441–448. [PubMed: 19770704]
28. An, YH.; Martin, KL. Handbook of histology methods for bone and cartilage. Humana Press; Totowa, NJ: 2003.
29. Maniatopoulos C, Rodriguez A, Deporter DA, Melcher AH. An improved method for preparing histological sections of metallic implants. Int J Oral Maxillofac Implants. 1986; 1:31–37. [PubMed: 3527956]
30. Martin RB. Determinants of the mechanical properties of bones. J Biomech. 1991; 24(Suppl 1):79–88. [PubMed: 1842337]
31. Ulrich D, van Rietbergen B, Laib A, Ruegsegger P. The ability of three dimensional structural indices to reflect mechanical aspects of trabecular bone. Bone. 1999; 25:55–60. [PubMed: 10423022]
32. Muller R, Van Campenhout H, Van Damme B, Van Der Perre G, Dequeker J, Hildebrand T, Ruegsegger P. Morphometric analysis of human bone biopsies: a quantitative structural comparison of histological sections and micro-computed tomography. Bone. 1998; 23:59–66. [PubMed: 9662131]
33. Cope JB, Samchukov ML. Regenerate bone formation and remodeling during mandibular osteodistraction. Angle Orthod. 2000; 70:99–111. [PubMed: 10832997]
34. Kabel J, Odgaard A, van Rietbergen B, Huiskes R. Connectivity and the elastic properties of cancellous bone. Bone. 1999; 24:115–120. [PubMed: 9951779]
35. Kinney JH. Connectivity and the elastic properties of cancellous bone. Bone. 1999; 25:741–742. [PubMed: 10593420]
36. Kinney JH, Ladd AJ. The relationship between three-dimensional connectivity and the elastic properties of trabecular bone. J Bone Miner Res. 1998; 13:839–845. [PubMed: 9610748]
37. Peltonen J. Bone formation and remodeling after symmetric and asymmetric physeal distraction. J Pediatr Orthop. 1989; 9:191–196. [PubMed: 2925853]
38. Vauhkonen M, Peltonen J, Karaharju E, Aalto K, Alitalo I. Collagen synthesis and mineralization in the early phase of distraction bone healing. Bone Miner. 1990; 10:171–181. [PubMed: 2224204]
39. Kuhn JL, Goldstein SA, Feldkamp LA, Goulet RW, Jesion G. Evaluation of a microcomputed tomography system to study trabecular bone structure. J Orthop Res. 1990; 8:833–842. [PubMed: 2213340]
40. Feldkamp LA, Goldstein SA, Parfitt AM, Jesion G, Kleerekoper M. The direct examination of three-dimensional bone architecture in vitro by computed tomography. J Bone Miner Res. 1989; 4:3–11. [PubMed: 2718776]
41. Ruegsegger P, Koller B, Muller R. A microtomographic system for the nondestructive evaluation of bone architecture. Calcif Tissue Int. 1996; 58:24–29. [PubMed: 8825235]
42. Hildebrand T, Ruegsegger P. Quantification of bone microarchitecture with the structure model index. Comput Methods Biomech Biomed Engin. 1997; 1:15–23. [PubMed: 11264794]
43. Hildebrand T, Laib A, Muller R, Dequeker J, Ruegsegger P. Direct three-dimensional morphometric analysis of human cancellous bone: microstructural data from spine, femur, iliac crest, and calcaneus. J Bone Miner Res. 1999; 14:1167–1174. [PubMed: 10404017]

NIH-PA Author Manuscript
NIH-PA Author Manuscript
NIH-PA Author Manuscript

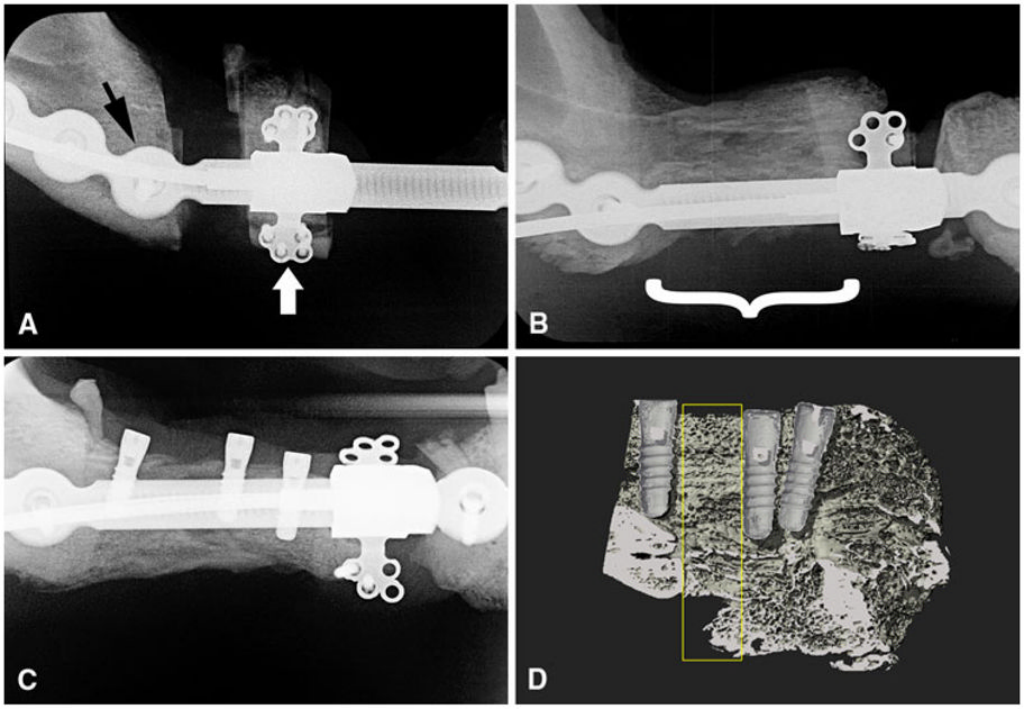

Fig. 1.

Radiographs of the experimental side of the mandible. The distraction vector is from posterior to anterior (from left to right in the figure). **a** Progress of the distraction osteogenesis after 1 week of device activation. The reconstruction plate (*black arrow*) is used to stabilize the mandible. The intraoral transport unit (*white arrow*) is attached both to the bone transport segment and to the reconstruction plate. **b** The regenerated bone (*bracket*) after 6 weeks of consolidation. **c** Dental implants placed in the regenerated bone. **d** Medium-resolution micro-CT image of the 18-week regenerated bone (sagittal plane) showing the implants and the lingual segment of the regenerated bone. *Yellow rectangle* indicates the VOI of the 3D analysis

NIH-PA Author Manuscript
NIH-PA Author Manuscript
NIH-PA Author Manuscript

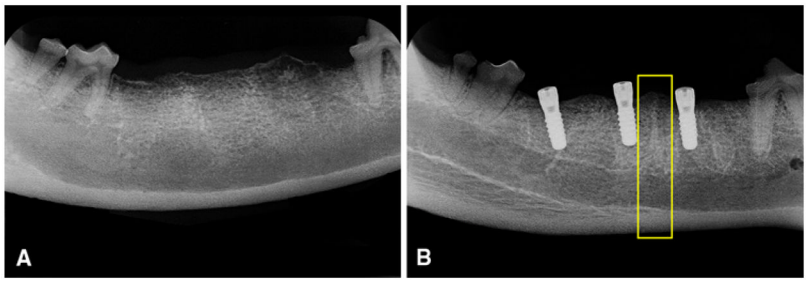

Fig. 2.
Radiographs of the control side of the mandible. **a** After extraction of the teeth. **b** After placement of dental implants. *Yellow rectangle* indicates the VOI of the 3D analysis between two implants

NIH-PA Author Manuscript
NIH-PA Author Manuscript
NIH-PA Author Manuscript

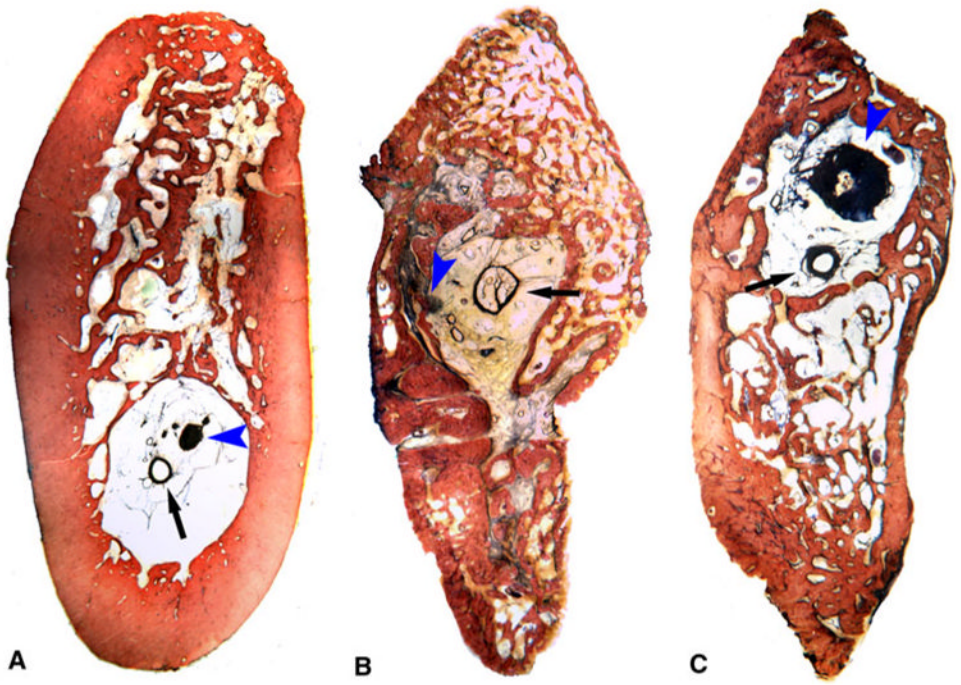

Fig. 3.

Histologic section of undecalcified tissues, photographed at 1× magnification. Blood vessels (*black arrows*) and nerves (*blue arrowheads*) were identified in all sections. **a** Control tissue at 12 weeks. **b** Regenerate tissue at 12 weeks. **c** Regenerate tissue at 18 weeks

NIH-PA Author Manuscript

NIH-PA Author Manuscript

NIH-PA Author Manuscript

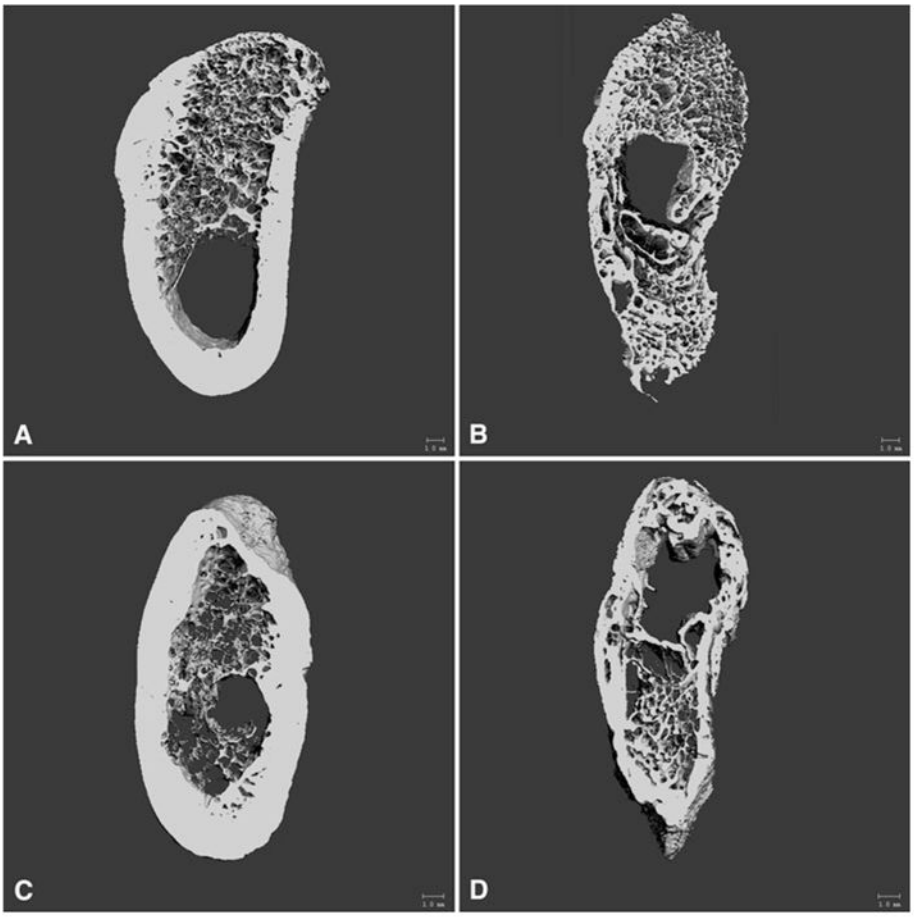

Fig. 4.
Micro-CT images of the whole VOI after reconstruction of the tomographic slices with a uniform threshold value. **a** Control tissue at 12 weeks. **b** Regenerate tissue at 12 weeks. **c** Control tissue at 18 weeks. **d** Regenerate tissue at 18 weeks

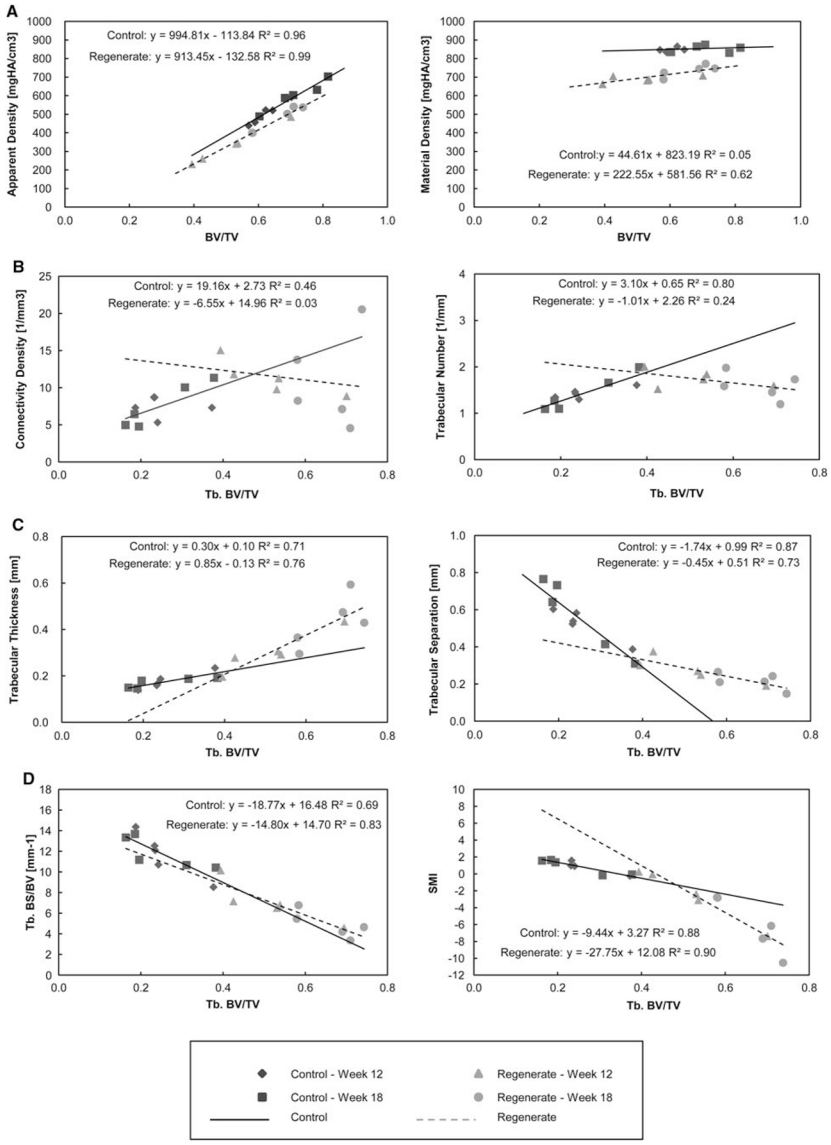

Fig. 5.

Regression analysis of micro-CT bone indices against bone volume fraction. Refer to Table 2 for statistical significance of the regression analyses

NIH-PA Author Manuscript
NIH-PA Author Manuscript
NIH-PA Author Manuscript

NIH-PA Author Manuscript
NIH-PA Author Manuscript
NIH-PA Author Manuscript

Calcif Tissue Int. Author manuscript; available in PMC 2012 July 1.

Table 1

Micro-CT results of control vs. regenerated bone (mean ± SD)

Bone index	Week 12		Week 18		Week[a]	Tissue type[b]	Tissue type*week[c]
	Control	Regenerate	Control	Regenerate	*P*≤	*P*≤	*P*≤
Apparent density (mgHA/cm^3)	506.03 ± 60.71	333.71 ± 98.88	602.96 ± 77.76	476.36 ± 71.00	0.036	0.000	0.127
Material density (mgHA/cm^3)	853.31 ± 14.62	689.89 ± 18.53	852.99 ± 19.07	735.19 ± 31.28	0.051	0.000	0.047
Bone volume (mm^3)	366.54 ± 49.51	139.74 ± 54.73	306.03 ± 47.72	323.24 ± 180.51	0.260	0.025	0.013
Total volume (mm^3)	585.02 ± 54.35	296.23 ± 151.42	425.52 ± 42.87	475.91 ± 231.90	0.888	0.072	0.018
BV/TV (%)	63 ± 5	52 ± 12	72 ± 8	66 ± 7	0.051	0.002	0.211
Tb.BV/TV (%)	25 ± 7	52 ± 12	25 ± 9	66 ± 7	0.253	0.000	0.004
Tb.BS/BV (1/mm)	11.66 ± 2.18	7.06 ± 2.00	11.87 ± 1.54	4.9 ± 1.30	0.404	0.000	0.001
Trabecular thickness (mm)	0.18 ± 0.04	0.30 ± 0.09	0.17 ± 0.02	0.43 ± 0.11	0.162	0.000	0.022
Trabecular separation (mm)	0.53 ± 0.08	0.28 ± 0.07	0.57 ± 0.20	0.22 ± 0.04	0.888	0.000	0.273
Trabecular number (1/mm)	1.43 ± 0.12	1.74 ± 0.19	1.42 ± 0.39	1.59 ± 0.29	0.409	0.137	0.626
Connectivity density (1/mm^3)	7.48 ± 1.39	11.37 ± 2.37	7.52 ± 3.00	10.85 ± 6.38	0.900	0.049	0.863

[a] Week is the test of between-subjects effect of consolidation time (Week 12 vs. Week 18)

[b] Tissue type is the test of within-subjects effect of distraction osteogenesis (Control vs. Regenerate)

[c] Tissue type*week is the test of the Interactive effect of distraction osteogenesis and consolidation time

BV/TV total bone volume fraction, *Tb. BV/TV* trabecular bone volume fraction, *Tb. BS/BV* trabecular bone surface ratio

NIH-PA Author Manuscript
NIH-PA Author Manuscript
NIH-PA Author Manuscript

Table 2

Regression of micro-CT bone indices against volume fraction

Bone index vs. volume fraction	Control	Regenerate
Apparent density vs. BV/TV		
Intercept	−113.91	−132.58
Slope	994.92	913.45
R^2	0.96	0.99
$P\leq$	0.000	0.000
Material density vs. BV/TV		
Intercept	823.17	581.56
Slope	44.63	222.55
R^2	0.05	0.62
$P\leq$	0.526	0.007
Tb. BS/BV vs. Tb. BV/TV		
Intercept	16.52	14.73
Slope	−19.09	−14.86
R^2	0.69	0.83
$P\leq$	0.003	0.000
Connectivity density vs. Tb.BV/TV		
Intercept	2.73	14.96
Slope	19.16	−6.55
R^2	0.46	0.03
$P\leq$	0.032	0.632
Trabecular number vs. Tb.BV/TV		
Intercept	0.64	2.27
Slope	3.15	−1.04
R^2	0.80	0.25
$P\leq$	0.001	0.138
Trabecular thickness vs. Tb.BV/TV		
Intercept	0.10	−0.13
Slope	0.31	0.85
R^2	0.71	0.77
$P\leq$	0.002	0.001
Trabecular separation vs. Tb.BV/TV		
Intercept	0.99	0.51
Slope	−1.77	−0.45
R^2	0.87	0.72
$P\leq$	0.000	0.002